Author for correspondence:
M. Taverne
e-mail: maxime.taverne@mnhn.fr

THE ROYAL SOCIETY
PUBLISHING

Form–function relationships underlie rapid dietary changes in a lizard

M. Taverne[1], P. J. Watson[2], H. Dutel[2,3], R. Boistel[1], D. Lisicic[4], Z. Tadic[4], A-C. Fabre[5,6,7], M. J. Fagan[2,†] and A. Herrel[1,5,†]

[1]UMR 7179, Département Adaptations du Vivant, Muséum National d'Histoire Naturelle, Centre National de la Recherche Scientifique, Paris, France
[2]Department of Engineering, University of Hull, Cottingham Road, Hull HU6 7RX, UK
[3]School of Earth Sciences, University of Bristol, 24 Tyndall Avenue, Bristol BS8 1TQ, UK
[4]Department of Biology, Faculty of Science, University of Zagreb, Rooseveltov trg 6, Zagreb, Croatia
[5]Naturhistorisches Museum der Burgergemeinde Bern, Bernastrasse 15, 3005 Bern, Switzerland
[6]Institute of Ecology & Evolution, Universität Bern, Baltzerstrasse 6, 3012 Bern, Switzerland
[7]Department of Life Sciences, Natural History Museum, London SW7 5BD, UK

MT, 0000-0003-3355-6200; PJW, 0000-0003-0220-2960; HD, 0000-0002-1908-5150; DL, 0000-0001-5587-6518; ZT, 0000-0002-7651-4425; A-CF, 0000-0001-7310-1775; AH, 0000-0003-0991-4434

Macroevolutionary changes such as variation in habitat use or diet are often associated with convergent, adaptive changes in morphology. However, it is still unclear how small-scale morphological variation at the population level can drive shifts in ecology such as observed at a macroevolutionary scale. Here, we address this question by investigating how variation in cranial form and feeding mechanics relate to rapid changes in diet in an insular lizard (*Podarcis siculus*) after experimental introduction into a new environment. We first quantified differences in the skull shape and jaw muscle architecture between the source and introduced population using three-dimensional geometric morphometrics and dissections. Next, we tested the impact of the observed variation in morphology on the mechanical performance of the masticatory system using computer-based biomechanical simulation techniques. Our results show that small differences in shape, combined with variation in muscle architecture, can result in significant differences in performance allowing access to novel trophic resources. The confrontation of these data with the already described macroevolutionary relationships between cranial form and function in these insular lizards provides insights into how selection can, over relatively short time scales, drive major changes in ecology through its impact on mechanical performance.

1. Introduction

Macroevolutionary changes such as changes in habitat use or diet are often associated with convergent, adaptive changes in morphology. Previous studies have suggested that for macroevolutionary changes to occur, directional selection driven by consistent changes in the environment is needed. Consequently, Carroll and colleagues [1] suggested that 'macroevolution may thus be nothing more than an aggregate of many small events'. Despite the initial assertion that macroevolutionary patterns cannot be predicted from processes at the population level [2], subsequent authors have demonstrated that patterns of variation among taxa can be predicted using population genetics theory [3]. Moreover, in some cases, variation in morphology can be rapid and may drive the subsequent evolutionary trajectory of a population [4]. Indeed, variation in fitness-relevant traits has the potential to rapidly drive a population across a valley of low fitness to a new adaptive peak [3,5–7], thus potentially driving rapid and seemingly punctuated changes in morphology [8,9]. Yet, for small-scale population-level variation to facilitate or drive rapid shifts in ecology and potentially allow organisms to reach these new adaptive peaks, this variation in morphology needs to have a significant impact on function. As the

link between morphology and function is often nonlinear [10], even small differences in form may potentially give rise to significant differences in function. For example, since the force output of a musculoskeletal system scales to the second power of linear dimensions, small changes in head dimensions can generate significant differences in bite force [11], which might in turn allow species to access novel resources [4,12–14].

Herbivory is an attractive ecological strategy that, at least in mammals, has resulted in fast species diversification [15] with over 38% of all mammals being considered herbivores [16]. By contrast to mammals, squamate herbivores are rare with merely 2% of all species being considered herbivores [17]. Among lizards this value may be as high as 5% [18], but herbivory remains an uncommon dietary niche. Among the reasons that have been suggested to have prevented lizards from becoming herbivorous are their small body size [19–21], unspecialized dentition [22] and lack of complex food processing [23]. However, it has since been demonstrated that even small lizards can be herbivorous [24] and that complex cusped teeth have evolved associated with an herbivorous diet [25]. Moreover, herbivorous lizards typically have higher bite forces than insectivorous species [13,26] which may allow them to crop leaves from a larger plant. The herbivorous niche in lizards thus appears to be an adaptive peak that is rather difficult to attain and needs to be accompanied by a suite of distinct anatomical and functional specializations.

A notable exception to the general idea that herbivory is difficult to achieve in lizards is the previously documented rapid evolution of a largely herbivorous diet in a population of Italian wall lizards (*Podarcis siculus*) roughly three decades after its introduction onto a small islet in the Adriatic [4,27]. Indeed, lizards that were introduced onto the islet of Pod Mrčaru from the neighbouring islet of Pod Kopište switched to a diet composed of up to 60% of plants in summer and show physiological adaptations, as well as differences in their microbiome, allowing them to more efficiently extract energy from a plant-based diet [4,28,29]. Moreover, in the 36 years since the introduction of these lizards on Pod Mrčaru, they developed larger heads, muscles, and bite forces and changed the shape of their cranium and mandible [4,30]. As the two islets are similar in size and show similar vegetation types and high lizard densities [4] the ecological drivers of the observed changes in diet remain unclear. Moreover, despite the documented changes in head shape and muscle architecture it remains unclear how these lizards were able to gain a great enough functional advantage to allow them to occupy a new adaptive peak in the fitness landscape (i.e. a plant-based diet). Here, we use dissections, geometric morphometrics, and mechanical engineering tools, including multibody dynamics analysis (MDA) and finite-element modelling (FEM), to better understand the functional advantages provided by the rather subtle changes in skull shape and muscle architecture previously documented in these two populations [30]. We demonstrate how an intricate coevolution of skull and mandible shape with muscle architecture can allow for a more efficient mechanical transfer of forces from the muscles to the jaws, and a more resistant skull configuration when biting. These results provide insights into how subtle phenotypic variation may give rise to fitness-relevant changes in function allowing the rapid transition towards new adaptive peaks and the occupation of novel trophic niches in lizards.

2. Material and methods

(a) Quantification and comparison of head shape and muscular anatomy

Thirteen male specimens from Pod Kopište and 14 male specimens from Pod Mrčaru were captured by hand or by noose at the end of the summer of 2013. Their body size (SVL: snout–vent length) and head size was measured with a Mitotoyo digital caliper (±0.01 mm) and their bite force was measured using a custom-designed bite force set-up [31]. They were sacrificed by an intramuscular injection of pentobarbital under a permit of the Croatian Ministry of the Environment. Specimens were preserved in a 10% aqueous formaldehyde solution for 48 h, rinsed and stored in a 70% aqueous ethanol solution.

The heads of these 27 specimens were scanned at the University of Poitiers on an Easytom micro-CT (at a voxel size of 24.90 µm with the following parameters: X-ray voltage, 90 kV; X-ray intensity, 70 µA; exposure time, 2000 ms; number of projections, 2500). Scans were imported into Avizo 9.0 (Thermo Fisher Scientific) to segment the mandible and skull which were exported as PLY files. A set of landmarks and semi-landmarks on curves were used to quantify the skull and mandible shape (see [30]; electronic supplementary material, figure S1 and table S1). Semi-landmarks on curves were slid while minimizing the bending energy and all landmarks were aligned by a Procrustes superimposition with the function 'gpagen' ('geomorph' package). The function 'prcomp' from the *stats* package was used to run a principal component analysis (PCA) on the Procrustes coordinates. A MANOVA on the principal components (PC) cumulatively explaining at least 85% of the variance was run to test for shape differences between populations. The theoretical shapes corresponding to the extremes of the PCs that distinguish populations were visualized using the functions 'tps3d' and 'shade3d' ('Morpho' package).

Five additional male specimens per population were included to quantify variation in jaw muscle architecture (resulting in a total 18 specimens from Pod Kopište and 19 specimens from Pod Mrčaru). Each muscle bundle was extracted by dissecting the left side of the head. Muscle bundles were blotted dry and weighed with a digital balance (Mettler AE100; ± 0.1 mg). The connective tissue surrounding the muscles was digested by submerging the muscles in a 30% aqueous nitric acid solution for 24 h. Next, the nitric acid was removed, and a 50% glycerol solution was added to arrest the muscle digestion. Muscle fibres were drawn under a binocular scope (Leica) with *camera lucida* (see [30]) and measured using Image J [32]. Muscle volume was calculated as the ratio between muscle mass and muscle density (1.06 g cm^{-3}; see [33]). The physiological cross-sectional area (PCSA) of each muscle bundle was subsequently calculated by dividing muscle volume by the mean fibre length and was subsequently corrected for pennation angle. The muscles were grouped into four functional groups: the external adductors, the pseudotemporalis group, the adductor posterior and the pterygoid group (electronic supplementary material, table S2). The jaw depressors and the constrictor dorsalis muscles were not considered since they are not involved in jaw closing.

Differences in the muscular architecture (muscle volume, PCSA, fibre length) between populations were tested by means of a multivariate analysis of covariance (MANCOVA) with the island as factor and SVL as co-variable, using the function 'mancova' from the package 'jmv'. Subsequent univariate ANOVAs were used to test which muscle groups were responsible for the observed differences.

(b) Multibody dynamics model design

The skull and the mandible of two males of similar size, one from the island of Pod Kopište (PK), one from Pod Mrčaru (PM), were

Table 1. Muscle architecture data used as input for the MDA models.

muscle	pennation	number of bundles	Pod Kopište			Pod Mrčaru		
			PCSA (mm^2)	muscle force (N)	force by bundle (N)	PCSA (mm^2)	muscle force (N)	force by bundle (N)
AMESA	15°	5	2.33	0.93	0.19	4.95	1.98	0.40
AMESP	18°	5	2.71	1.09	0.22	3.51	1.40	0.28
AMEM	11°	11	2.80	1.12	0.10	2.84	1.13	0.10
AMEP	41°	9	0.82	0.33	0.04	0.79	0.32	0.04
AMP	21°	4	0.99	0.40	0.10	1.61	0.64	0.16
PSTS	27°	5	1.70	0.68	0.14	2.20	0.88	0.18
PSTP	0°	6	4.13	1.65	0.28	4.65	1.86	0.31
PTL	30°	7	2.70	1.08	0.15	4.44	1.77	0.25
PTM	0°	5	4.93	1.97	0.39	5.47	2.19	0.44

segmented using Avizo 9.0 (Thermo Fisher Scientific). The three-dimensional models of the cranium and jaw of each specimen were used to build two MDA models. The location of the origin and insertion of each jaw muscle was assessed based on dissections and each muscle was virtually divided into several distinct muscle bundles according to the size of the muscle. The number of bundles used was based on the muscle volume and area of insertion (table 1). The coordinates of the sites of origin and insertion of each muscle bundle were determined using Avizo 9.0 (Thermo Fisher Scientific). The mandible was converted into a parasolid format allowing to compute the inertial properties based on a bone density of 1.5 g cm^{-3} [34]. The skull surface, the mandible parasolid and the muscle bundle coordinates were imported into MSC ADAMS multibody dynamic simulation software (Santa Ana, CA, USA). The muscle bundles were modelled as contractile springs. Where necessary, muscle bundles were wrapped around the bone to increase the accuracy of modelling [35] (figure 1). Muscle PCSAs were corrected by both the pennation angle and the typical 10% loss in muscle volume due to tissue preservation [36]. The maximum force of each muscle (table 1) was calculated by multiplying the PCSA by an intrinsic muscle stress of 40 N cm^{-2} [35]. The MDA models simulated opening and closing of the jaw assuming maximal activation of the bundles when the system was at equilibrium. A food particle was created and aligned perpendicularly to the toothrow of the upper jaw to generate a reaction force due to jaw closing (simulated bite force). To ensure consistency in the output bite force generated by the MDA models, the location of the contact between the food particle and the teeth was prescribed to match the location of the contact between the teeth and the plates of the force transducer used to measure *in vivo* bite force in the field [37]. To run further simulations, the location of the item was then standardized at the middle of the maxillary toothrow, as observations revealed that lizards typically crush prey at that location [38]. The stiffness of the food particle was intentionally set beyond the hardness of prey typically consumed by the lizards to ensure that the gape angle did not change during a biting simulation and to obtain the maximal bite force.

(c) Finite-element model design

Two finite-element meshes consisting of about 1.5 million tetrahedral elements (PK: 1 527 268 elements; PM: 1 321 278 elements) were generated in Avizo and imported into ANSYS (ANSYS, Canonsburg, PA, USA) for finite-element analysis. Bone was assumed to have isotropic homogeneous material properties with a Young's modulus of 17 GPa and a Poisson's ratio of 0.3 [39,40]. The meshes were constrained at the ventral base of the quadrates (the right side in all three directions, the left in A-P and D-V only) and at two symmetrical bite points in the D-V direction (figure 1). The coordinates of these locations were directly exported from ADAMS, with the three-dimensionally resolved forces exported from the MDA solutions then directly applied onto the skull model. The quadrato-jugal and the epipterygoid-parietal ligaments were modelled as tension-only links with a stiffness of 250 N mm^{-2} and a cross-sectional area of 1 mm^2 (electronic supplementary material, figure S2). Sensitivity tests were carried out using the Pod Kopište model biting at a 20° gape to quantify the impact of the presence/absence and variation in stiffness of the ligaments (50, 250 and 500 N mm^{-2}) on the stress distribution (electronic supplementary material, figures S3 and S4). The stress values associated with each element of the mesh were exported into an element table for postprocessing.

(d) Simulations

Four different MDA and FEA models were built: two 'natural' models in which the specimens were modelled with their own musculature (PK_PK and PM_PM); and two 'theoretical' models in which muscle PCSAs were swapped (i.e. PK_PM: the morphology of Pod Kopište with the musculature of Pod Mrčaru, and PM_PK the morphology of Pod Mrčaru with the musculature of Pod Kopište). These models allowed us to test the impact of changes in cranial morphology and muscle anatomy on the calculated bite force by comparing the results of the simulations. The bite force in each of the four models was calculated for 10 different gape angles, from 0° (closed jaw) to 45° (maximum gape typically attained at the onset of fast closing [38]), thereby effectively varying the size of the prey item. For each MDA model, the conversion rate of the total muscle force into bite force was calculated at every gape tested by dividing bite force by the total muscle force and was used to assess the efficiency of a muscle to translate intrinsic muscle force into bite force. The total amount of change in bite force between the two natural models was quantified as it provides direct information on how much the mechanical properties of the masticatory system of the two specimens differ. The amount of change in bite force due to the change in muscle anatomy or to the change in cranial morphology alone was also quantified. This allowed us to estimate the relative contribution (in %) of changes in cranial morphological or in muscular
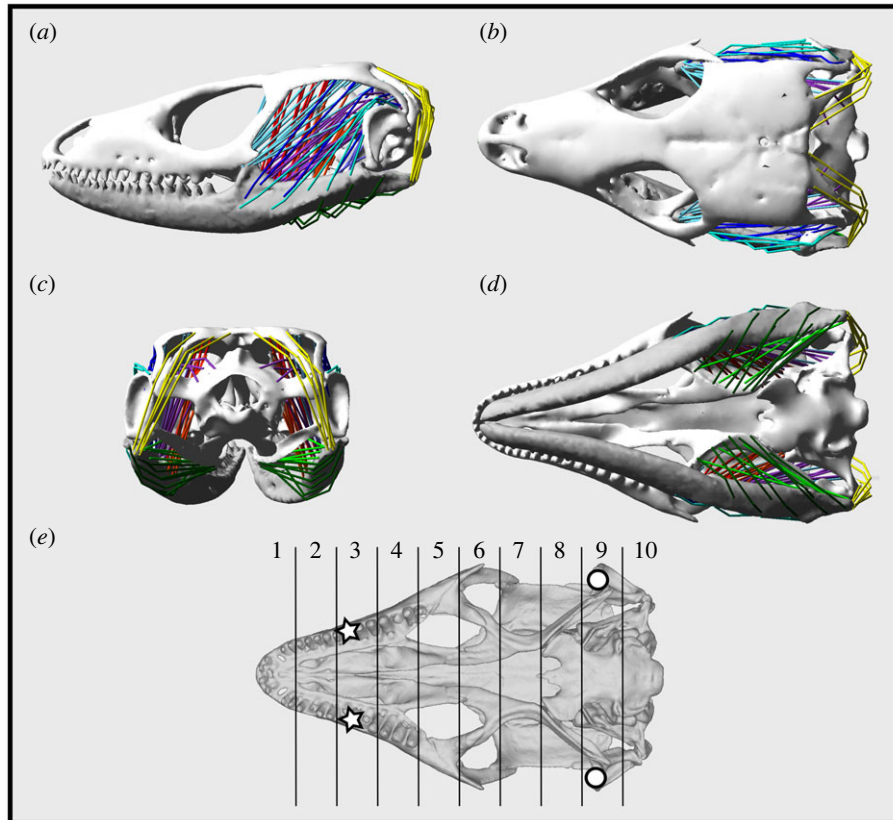
Figure 1. MDA model design illustrating the muscle bundles used of each muscle and their wrapping. (*a*) Left lateral view of the skull. (*b*) Dorsal view. (*c*) Caudal view. (*d*) Ventral view. The jaw opener is represented in yellow, the external adductors in shades of blue, the pseudotemporalis in red and orange and the pterygoids in green. (*e*) Segments of the skull used to investigate the variation in stress accumulation over the structure (here represented by a ventral view) in subsequent FEA. Note that the bite points and the joints are indicated by white stars and white circles, respectively.

anatomy to generate the observed differences in bite force between the specimens. The role of each muscle in bite force generation was assessed by running MDAs with only one muscle activated at a time.

The results of the MDA models were then imported into ANSYS, after having been multiplied by five to obtain realistic absolute loads corresponding to *in vivo* bite forces (i.e. the calculated bite forces were five times lower than the *in vivo* forces). For each model, FEAs were performed at three gape values that mimicked three ecologically relevant scenarios: biting a thin object like a leaf (0°), biting a prey of medium size (20°) and biting a large prey item or a conspecific during for example male-male interactions (45°). Values of stress in each skull element were saved. Specifically, we focused on the von Mises stress (vMS) and recorded the mean stress values for the whole skull and the variation in the stress along the skull. To do so we divided the geometry into 10 segments of equal length (figure 1) and averaged the vMS values within each section. We then calculated the 'advantage' of the PM morphology relative to the PK morphology as the percentage of increase/decrease of the mean vMS accumulation along the skull. Finally, we estimated the homogeneity of the distribution of stress by calculating the Shannon's entropy [41] based on the density distribution of vMS values. A higher entropy reflects a low redundancy and a high disparity in the data. Thus, the 'advantage' provided by the PM morphology was estimated as the proportional difference in entropy between the two models.

3. Results

(a) Morphological differences

Lizards from the two islets differ in snout-vent length (Pod Kopište: 62.3 ± 3.7 mm for males; 58.2 ± 3.0 mm for females;

Pod Mrčaru: 68.3 ± 3.2 mm for males; 62.72 ± 2.9 for females), head length (Pod Kopište: 14.9 ± 0.7 mm for males; 13.0 ± 0.6 mm for females; Pod Mrčaru: 16.22 ± 0.8 mm for males; 13.8 ± 0.6 for females), and bite force (Pod Kopište: 17.3 ± 4.6 N for males and 9.6 ± 1.9 N for females; Pod Mrčaru: 27.01 ± 3.2 N for males and 14.8 ± 2.7 N for females).

The MANOVA including the first nine axes of the PCA carried out on skull shape (cumulative variance: 85.2%) revealed an effect of island (Wilks' lambda = 0.22; $F_{1,25} = 6.861$; $p < 0.001$), especially on PC3 (variance = 9.3%; $F_{1,25} = 26.48$; $p < 0.001$) and PC6 (variance = 3.3%; $F_{1,25} = 4.83$; $p = 0.037$). The theoretical shape deformation along PC3 showed that the population of PM had a slightly shorter snout and a more curved quadrate (electronic supplementary material, figure S5). The MANOVA including the first 9 axes of the PCA carried out on mandible shape (cumulative variance: 85.0%) also revealed an effect of island (Wilks' lambda = 0.40; $F_{1,25} = 2.86$; $p = 0.029$), especially along PC1 (variance = 24.4%; $F_{1,25} = 7.50$; $p = 0.011$). The theoretical shape deformation along PC1 showed that the mandible of the PM population was overall more ventrally curved (electronic supplementary material, figure S5). The coronoid was medially and caudally thicker, the lateral crest, which serves as the insertion site of external adductors was wider, the retroarticular process shorter, and the joint surface area larger.

The MANCOVA carried out on the muscle variables detected significant differences between islands (table 2). All variables (muscle mass, fibre length and PCSA) were greater in specimens from Pod Mrčaru. When accounting for body size, specimens from Pod Mrčaru had heavier external adductors and pterygoid muscles, shorter fibres in the

Table 2. Results of the multivariate analyses of covariance (MANCOVAs) testing for differences in muscle architecture (muscle mass, fibre length, and muscle PCSA) between the two lizards from Pod Kopište and Pod Mrčaru, with the snout–vent length (SVL) as covariable. F: F-statistic, d.f.: degrees of freedom. p-values smaller than 0.05 are considered significant and are indicated with an asterisk.

	Wilks's lambda	F	hypothesis d.f.	error d.f.	p	
mass	0.423	10.55	4	31	<0.001*	SVL
	0.636	4.44	4	31	0.006*	island
length	0.542	6.54	4	31	0.001*	SVL
	0.531	6.64	4	31	0.001*	island
PCSA	0.455	9.28	4	31	<0.001*	SVL
	0.667	3.88	4	31	0.011*	island

Table 3. Results of the univariate analyses of covariance (ANCOVAs) testing for differences in muscle architecture (muscle mass, fibre length and muscle PCSA) between lizards from Pod Kopište (PK) and Pod Mrčaru (PM), with the snout–vent length (SVL) as covariable and for each muscle group separately. Significant results are indicated with an asterisk, in which cases bold values indicate which population has the highest mean values. .

variable	muscle group	mean square	F	sigma	mean (PK)	mean (PM)
mass	**ADD**	0.087	16.73	<0.001*	1.424 ± 0.022	**1.572 ± 0.021**
	PST	0.004	0.85	0.364	1.100 ± 0.020	1.130 ± 0.019
	PTG	0.115	17.54	<0.001*	1.355 ± 0.025	**1.525 ± 0.024**
	AMP	0.021	0.96	0.333	0.365 ± 0.045	0.437 ± 0.043
length	ADD	0.003	0.81	0.375	0.366 ± 0.018	0.340 ± 0.017
	PST	0.001	0.49	0.488	0.366 ± 0.017	0.385 ± 0.016
	PTG	0.004	1.75	0.195	0.341 ± 0.014	0.371 ± 0.013
	AMP	0.088	8.29	0.007*	**0.338 ± 0.032**	0.189 ± 0.030
PCSA	**ADD**	0.105	11.99	0.001*	1.027 ± 0.029	**1.190 ± 0.028**
	PST	0.001	0.05	0.825	0.703 ± 0.018	0.709 ± 0.017
	PTG	0.071	8.97	0.005*	0.993 ± 0.027	**1.127 ± 0.026**
	AMP	0.195	9.97	0.003*	0.001 ± 0.043	**0.223 ± 0.041**

AMP, and a greater PCSA of the external adductors and the AMP (table 3).

(b) Mechanical basis of variation in bite force

The MDAs showed that models with the musculature of the PM specimen always resulted in higher bite forces, and that models with the shape of PM individuals resulted in higher bite forces irrespective of variation in muscle architecture (figure 2; table 4). This held irrespective of the gape tested, and was even exacerbated with an increase in gape. Simulated bite force reached two peaks in the four models, at closed gapes (0° or 5° in PK_PM) and wide gapes (45°) and was minimal at a gape of around 30°/35°. Knowing that the total bite force of the PK and the PM individuals modelled in the present study was 19.1 N and 25.0 N respectively, the simulations showed that the conversion rate of the PM morphology is always higher than in the PK morphology (figure 2). The total amount of change in simulated bite force between the two natural models varied between 30.5% (0°) and 37.5% (40°). On average, the relative contribution from the change in skull shape to total variation in bite force increased with gape and varied between 2.41% (5°) and 12.49% (45°), the remainder being explained by variation in muscle architecture (figure 3).

In all models, the external adductors contributed the most to bite force (on average approximately 50%), then the pseudotemporalis (35%), and the pterygoids (15%) (electronic supplementary material, figures S6 and S7, electronic supplementary material, table S3). The relative contribution of the muscles varied with gape; the contribution of the external adductors decreased with gape, while that of the pterygoid increased. The pseudotemporalis group had the highest conversion rate of muscle force into bite force (approx. 30% on average), followed by the external adductors (22%) and the pterygoids (12%) (electronic supplementary material, figure S7). The conversion rate of the adductors decreased with gape in all models, while the conversion rate of the pterygoids increased, and that of the pseudotemporalis decreased from gape 0° to 30° and increased from 30° to 45°. Compared to the morphology of PK, the PM morphology was associated with higher conversion rates of the adductors for all gapes, of the pseudotemporalis for gapes wider than 10°, and for the pterygoids for gapes wider than 30°.

(c) Structural performance of the skull

The comparison of the two natural models showed that, on average, the von Mises stress magnitude (vMS) in the cranium of PM_PM model was higher than in the PK_PK model
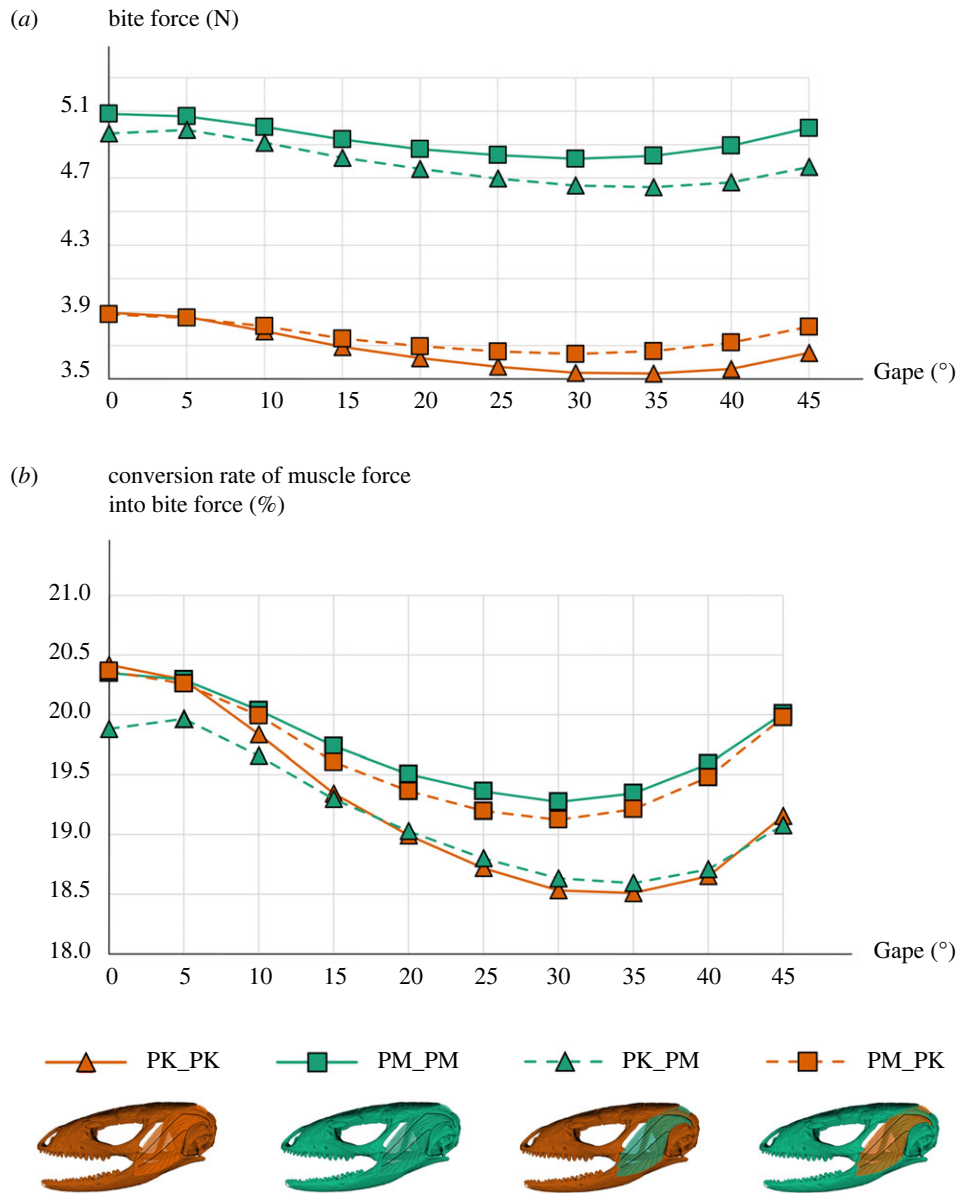
Figure 2. (*a*) Relationship between bite force (in Newtons), estimated by the MDA for the four models, and the gape (in degrees). (*b*) Relationship between the conversion rate of the total muscle force into bite force (in percentage) and the gape (in degrees) for all models. The two natural models (PK_PK: including the morphology and the musculature of Pod Kopište, PM_PM: including the morphology and the musculature of Pod Mrčaru) are represented by full lines, whereas the two hybrid models (PK_PM: including the morphology of Pod Kopište and the musculature of Pod Mrčaru, PM_PK: including the morphology of Pod Mrčaru and the musculature of Pod Kopište) are represented by dashed lines.

(from 6% to 17%) (figure 4). Although PM_PM showed lower vMS magnitudes (except for the two most posterior sections of the skull) at a 0° gape, more stress was detected at 20° and 45°. Interestingly, the amount of vMS observed significantly increased with gape in PM_PM, whereas this was not the case in PK_PK. Specifically, the increase in vMS in the PM_PM natural model affected the whole skull (figure 4). An increase of 2% to 6% was also observed in the overall entropy in the PM_PM model (table 5).

The PM morphology enabled the mean vMS to decrease by 15% compared to a PK skull model with the PM musculature. The advantage provided by the PM morphology, estimated in percentage of loss in vMS, increased at low gape and was more pronounced in the anterior part of the skull than the posterior part (figure 5). Indeed, the advantage of a PM morphology was 13% to 41% in the snout, 9% to 20% in the region of the jugal, and became null or

slightly negative in the two most posterior regions (where stress magnitude increased). Specifically, the unloading allowed by the PM skull morphology concerned the maxilla, the vomer, the frontal, the anterior part of the pterygoid, the epipterygoid, the parietal and the quadrate. On the contrary, the areas that showed higher stress magnitudes included the wings of the prootic and the posterior tip of the pterygoid. Although less obvious when reaching a 45° gape, this pattern of stress distribution was similar at all gapes (figure 5). On average, the vMS magnitude increased (from 19% at 0° to 27% at 45°) when a PM musculature rather than a PK musculature was applied to a given morphology. In all cases, the overall level of entropy increased when a PM musculature rather than a PK musculature was applied on a given morphology (from 6% at 0° to 7% at 45°). The PM morphology provided only a small advantage in reducing overall entropy (differences < 5%; table 5).

Table 4. In silico bite forces calculated by the MDA simulations (in N), depending on the gape (in degrees), for all four models (PK_PK: including the morphology and the musculature of Pod Kopište, PM_PM: including the morphology and the musculature of Pod Mrčaru, PK_PM: including the morphology of Pod Kopište and the musculature of Pod Mrčaru, PM_PK: including the morphology of Pod Mrčaru and the musculature of Pod Kopište). On the right are indicated the associated conversion rate of muscle force into bite force (in percentage).

gape	simulated bite force (N)				force conversion rate (%)			
	PK_PK	PM_PM	PK_PM	PM_PK	PK_PK	PM_PM	PK_PM	PM_PK
0	3.90	5.08	4.97	3.89	20.42	20.35	19.88	20.37
5	3.87	5.07	4.99	3.87	20.29	20.29	19.97	20.26
10	3.79	5.01	4.91	3.82	19.84	20.04	19.66	19.99
15	3.69	4.93	4.82	3.74	19.34	19.74	19.30	19.61
20	3.62	4.87	4.75	3.70	18.99	19.51	19.03	19.36
25	3.57	4.84	4.70	3.66	18.72	19.36	18.80	19.20
30	3.54	4.82	4.66	3.65	18.53	19.27	18.63	19.12
35	3.53	4.83	4.65	3.67	18.51	19.35	18.59	19.21
40	3.56	4.89	4.67	3.72	18.65	19.59	18.71	19.48
45	3.66	5.00	4.77	3.81	19.16	20.01	19.08	19.98

4. Discussion

A significant difference in cranial anatomy and muscle architecture exists between the individuals from Pod Kopište and Pod Mrčaru. The latter showing stronger jaw adductors associated with their larger size and omnivorous diet. Lizards from Pod Mrčaru are bigger than those from Pod Kopište, but the variation in muscle cross-sectional area is not only due to differences in size. This is in line with the results of a previous study comparing multiple populations of *Podarcis* lizards [30]. Our results suggest that other factors may impact the differences in muscle architecture. For example, lizards from Pod Mrčaru have stronger pterygoid muscles which have a low moment arm at low gape [31,42]. As plant consumption typically involves biting at low gape, this suggests that diet might not underpin the differences in the cross-sectional area of pterygoid muscles observed between lizards from the two populations. We rather suggest that biting in the context of intraspecific interactions may better explain this difference. The density of lizards on Pod Mrčaru is roughly five times higher than on Pod Kopište [4,43], increasing the probability of encounters and aggressive interactions. Biting congeners involves biting at large gape which may drive the observed differences in the pterygoid muscle [44]. Populations also differed in cranial and mandibular shape. Our results show that lizards on Pod Mrčaru have a mandible that is more ventrally curved, with a wider lateral insertion area for adductor muscles, and a more robust coronoid. The results for skull morphology are less clear and mainly show differences in the curvature of the quadrate and a shorter snout in animals from Pod Mrčaru. The fact that the morphological differences in the cranium are less clear is likely a consequence of the multiple functions that the cranium fulfills (e.g. protection of the central nervous system and of the sensory organs), and the associated constraints and trade-offs. Non-adaptive processes including founder effects or genetic drift after introduction may also have driven the phenotypic differences between the two populations observed here [45].

Our modelling results demonstrate that differences in bite force between the two morphotypes are principally driven by the difference in the total muscle PCSA (table 2). The *in silico* estimates of bite force generated by the MDA simulations suggested that the lizards from Pod Mrčaru bite harder than those of Pod Kopište. Yet, subtle differences in cranium and mandible shape also contributed to the observed variation in bite force between the two populations. The comparison of the natural and hybrid models showed that the morphology of Pod Mrčaru enables greater bite forces to be generated in all cases. Moreover, the correlation between bite force and gape parallels the observed relation between conversion rate and gape (figure 2). Hence, variation in bite force at different gape angles depends on the proportion of muscle force converted into bite force, which in turn is impacted by head shape. This is further supported by the relative contribution of musculature and morphology to the differences in bite force. Consequently, the relatively subtle shape changes in the mandible and cranium between these two recently diverged populations are responsible for a considerable part of the variation in bite force. This is achieved by modulating the lever-arms associated with the muscle bundles that depend on the variation in skull and mandible geometry as well as differences in muscle size and cross-sectional area.

The comparison of the natural models PK_PK and PM_PM highlighted differences in structural performance between the phenotypes of the two populations and revealed that the phenotype of Pod Mrčaru accumulates more stress. Given that the PM model includes a greater total muscle PCSA, this is expected. Moreover, our models confirm that applying greater forces on a given morphology increases the level of VM stress over the skull. But the magnitude of differences in stress due to musculature is greater (19% to 27%) than that observed between the natural models (from 6% to 17%) suggesting that morphology itself might help dissipate stress. Indeed, the PM morphology conferred a clear advantage in dissipating stress compared to the PK morphology (figure 5). Similarly, the comparison of the natural
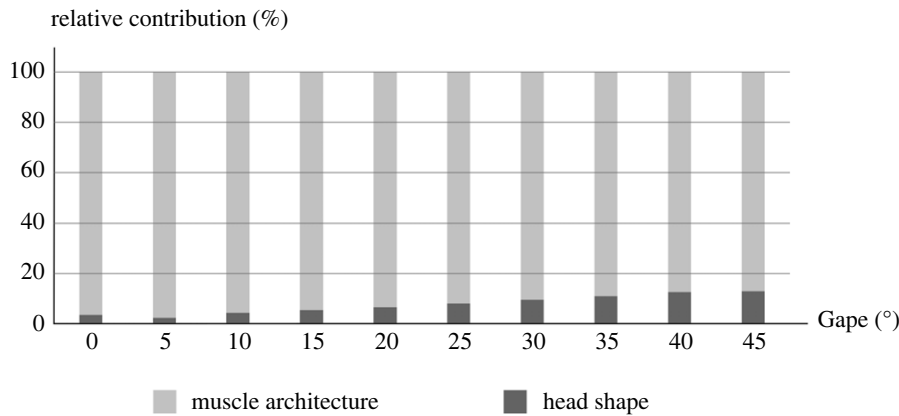
Figure 3. Contribution (in percent) of the differences in musculature (in light gray) and skull shape (in dark gray) in explaining the total difference in calculated bite force between individuals from the two islands (Pod Kopište and Pod Mrčaru). The contributions were estimated for every gape tested (in degrees) by comparing the change in calculated bite force induced by the change in musculature or morphology alone (theoretical models) with the change in calculated bite force between the two natural models.
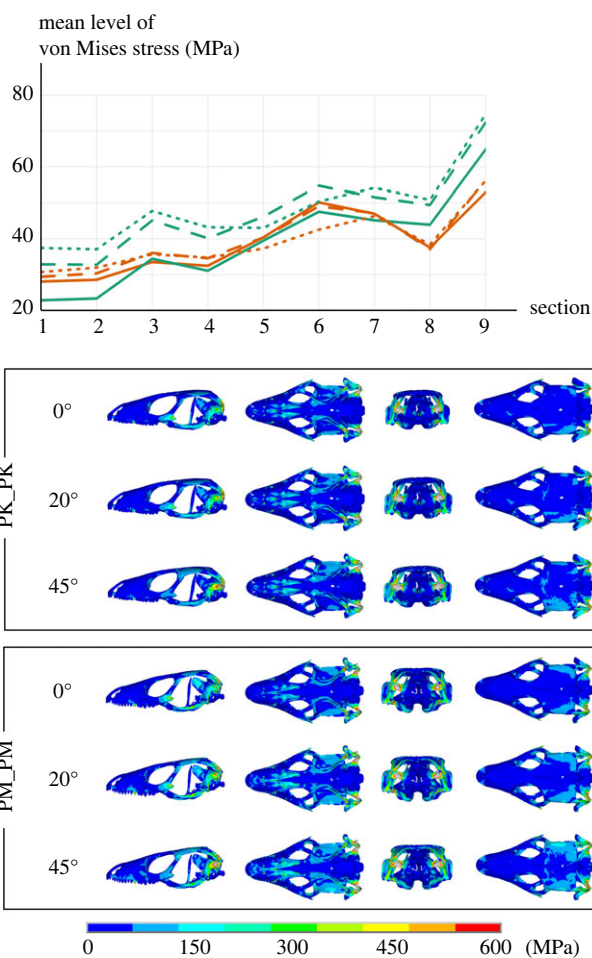
Figure 4. von Mises stress distribution in the two natural models (Brown lines: PK_PK, green lines: PM_PM) for the three gapes tested (full lines: 0°, dashed lines: 20°, dotted lines: 45°). Stresses are plotted relative to the virtual skull section number (i.e. position along the antero-posterior axis for which results were averaged; see methods). The left lateral, ventral, caudal and dorsal views of the skull are represented (from left to right). Warmer colours are associated with higher von Mises stress magnitudes (in MPa).

Table 5. Differences in entropy levels between finite-element simulations, depending on the gape (in degrees). The first column presents the increase in entropy level detected between the two natural models (PK_PK: including the morphology and the musculature of Pod Kopište, PM_PM: including the morphology and the musculature of Pod Mrčaru). The second column presents the increase in entropy level associated with a theoretical increase in the muscle forces. The third column presents the advantage conferred by the morphology of Pod Mrčaru (percentage of decrease in entropy level).

gape angle	PK_PK versus PM_PM	effect of musculature	advantage of PM morphology
0°	1.84%	5.51%	3.74%
20°	5.28%	6.89%	1.71%
45°	6.58%	7.35%	0.82%

with the application of a PM musculature to a given morphology leading to an overall increase in entropy (from 6% at 0° to 7% at 45°). Interestingly, our results suggest that an increase in the total muscle force is accompanied with an increased disparity in the distribution of the stress over the skull, yet the phenotype of Pod Mrčaru maintained a more homogeneous stress distribution.

Unexpectedly, the PM morphology was more advantageous than the PK morphology in producing bite force at wide gapes (as revealed by the MDA simulations), whereas it is more advantageous in dissipating stress at lower gapes (as revealed by the FEA simulations). Although this might first seem contradictory, we propose that these two results are not incompatible. We rather think that selection primarily acts upon the performance of the musculoskeletal system (i.e. bite force) within the limits imposed by the intrinsic capacity of the system to dissipate the associated stress and strain. Therefore, the MDA results suggest that the evolution of skull morphology towards a Pod Mrčaru phenotype enabled an optimization of bite force at wide gapes. This is probably driven by intraspecific competition, enhanced by a five-fold increase in population density on Pod Mrčaru [4,43]. The consumption of hard and fibrous material like plant matter requires repeated and frequent biting [46] to reduce the

models revealed that the phenotype of the Pod Mrčaru individuals had a greater level of overall entropy compared to that of Pod Kopište (from 2% at 0° to 6% at 45°). Again, this is mainly due to an increase in the total muscle force
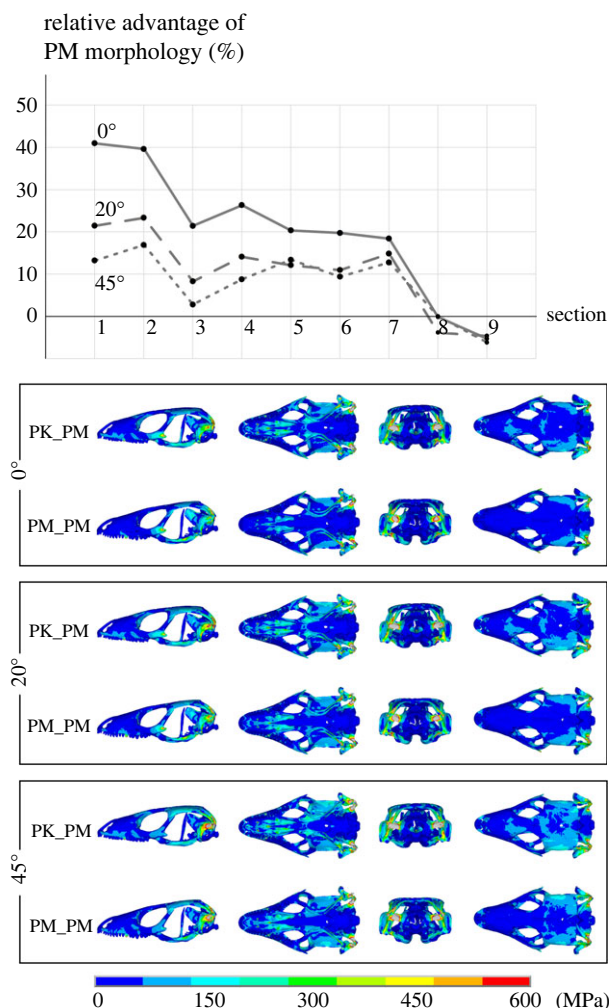
Figure 5. Consequences of skull shape change on the von Mises stress distribution. The graph represents the mean advantage (in %) provided by the PM morphology along the skull (full line: 0°, dashed line: 20°, dotted line: 45°). Here the models PK_PM and PM_PM (PK / Pod Kopište and PM / Pod Mrčaru in the figure) were compared for each of the three gapes tested (see electronic supplementary material, figure S8 for the alternative combination PM_PK versus PK_PK). Hotter colours are associated with higher von Mises stress magnitudes (in MPa).

item into smaller and more easily digestible bite-size pieces [47,48]. The structural advantage provided by the PM morphology at low gapes might be important in this context. Indeed, the repeated loading occurring at low gapes experienced by the skull while feeding on plants is likely to be particularly constraining and might represent an important selective agent driving variation in skull shape. A scenario in which head shape in insular *Podarcis* lizards is initially driven by intraspecific competition, and maintained by functional demands associated with resource use, would be in line with the results of Donihue *et al.* [44] concerning intraspecific variation in morphology and performance in another *Podarcis* species.

Previous comparative studies on the colonization of *Podarcis melisellensis* and *Podarcis siculus* in the Adriatic archipelago and their morphological evolution in relation to variation in ecological contexts [30,37,49] suggested that relationships between form and function were similar at different levels of integration, whether between isolated populations or between species, and even when accounting for phylogenetic relationships. Specifically, convergent

evolution of muscle architecture and head morphology were found in similar ecological contexts. Here, we demonstrate that these form–function relationships can evolve on ecological time scales and be associated with an optimization of the mechanical output of the masticatory system. Consequently, subtle morphological variation may accumulate over time and give rise to macroevolutionary patterns.

(a) Future directions

Further efforts might help make the finite-element models even more realistic and circumvent some of the current limitations. First, the simulations revealed an unrealistic accumulation of vMS at the very back of the skull (figures 4 and 5) at the most lateral region of the neurocranium (para-occipital process of the exoccipital). In the present study, the joint between the lateral process of the exoccipital and the quadrate was modelled as connected and fixed, hence possibly explaining why abnormal stress concentrations are located in this area instead of being more homogeneously distributed. It would be useful to model a ligamentous connection between these bones allowing a better stress dissipation. Second, bone tissue was modelled as an isotropic material here, although it is known to be anisotropic [50]. A precise quantification of the bony material properties throughout the skull (Young's modulus) should be undertaken using a nano-indentation approach. A third way to gain accuracy would be to model the sutures and the osteoderms, since they have been suggested to impact how loads are distributed and dissipated [51–53].

5. Conclusion

Our results show significant differences in skull form and function in individuals of two populations of *P. siculus*. Following the introduction into a novel environment, the population on Pod Mrčaru rapidly evolved a largely herbivorous diet. Our analyses of shape and function provide a mechanistic underpinning of the link between relatively subtle differences in morphology and the observed changes in ecology. Our results demonstrate that relationships between form and function may drive variation in fitness-relevant performance traits resulting in changes in trophic ecology over a relatively short time scale.

References

1. Caroll SP, Hendry AP, Reznick DN, Fox CW. 2007 Evolution on ecological timescales. *Funct. Ecol.* **21**, 387–393. (doi:10.1111/j.1365-2435.2007.01289.x)

2. Eldredge N, Cracraft J. 1980 *Phylogenetic patterns and the evolutionary process*. New York, NY: Columbia University Press.

3. Arnold SJ, Pfrender ME, Jones AG. 2001 The adaptive landscape as a conceptual bridge between micro- and macroevolution. *Genetica* **112–113**, 9–32. (doi:10.1023/A:1013373907708)

4. Herrel A, Huyghe K, Vanhooydonck B, Backeljau T, Breugelmans K, Grbac I, Van Damme R, Irschick DJ. 2008 Rapid large-scale evolutionary divergence in morphology and performance associated with exploitation of a different dietary resource. *Proc. Natl Acad. Sci. USA* **105**, 4792–4795. (doi:10.1073/pnas.0711998105)

5. Arnold SJ. 1983 Morphology, performance, and fitness. *Am. Zool.* **23**, 347–361. (doi:10.1093/icb/23.2.347)

6. Schluter D. 2000 *The ecology of adaptive radiation*. Oxford, UK: Oxford University Press.

7. Svensson EI, Calsbeek RE. 2012 *The adaptive landscape in evolutionary biology*. Oxford, UK: Oxford University Press.

8. Gingerich PD. 1983 Rates of evolution: effects of time and temporal scaling. *Science* **222**, 159–161. (doi:10.1126/science.222.4620.159)

9. Eldredge N. 1985 *Time frames: the evolution of punctuated equilibria*. Princeton, NJ: Princeton University Press.

10. Koehl MAR. 1996 When does morphology matter. *Annu. Rev. Ecol. Syst.* **27**, 501–542. (doi:10.1146/annurev.ecolsys.27.1.501)

11. Herrel A, O'Reilly JC. 2006 Ontogenetic scaling of bite force in lizards and turtles. *Physiol. Biochem. Zool* **79**, 31–42. (doi:10.1086/498193)

12. Aguirre LF, Herrel A, Van Damme R, Matthysen E. 2003 The implications of food hardness for diet in bats. *Funct. Ecol.* **17**, 201–212. (doi:10.1046/j.1365-2435.2003.00721.x)

13. Herrel A, Vanhooydonck B, Van Damme R. 2004 Omnivory in lacertid lizards: adaptive evolution or constraint? *J. Evol. Biol.* **17**, 974–984. (doi:10.1111/j.1420-9101.2004.00758.x)

14. Herrel A, Joachim R, Vanhooydonck B, Irschick DJ. 2006 Ecological consequences of ontogenetic changes in head shape and bite performance in the Jamaican lizard *Anolis lineatopus*. *Biol. J. Linnean Soc.* **89**, 443–454. (doi:10.1111/j.1095-8312.2006.00685.x)

15. Price SA, Hopkins SSB, Smith KK, Roth VL. 2012 Tempo of trophic evolution and its impact on mammalian diversification. *Proc. Natl Acad. Sci. USA* **109**, 7008–7012. (doi:10.1073/pnas.1117133109)

16. Atwood TB, Valentine SA, Hammill E, McCauley DJ, Maddin EMP, Beard KH, Pearse WD. 2020 Herbivores at the highest risk of extinction among mammals, birds, and reptiles. *Sci. Adv.* **6**, eabb8458. (doi:10.1126/sciadv.abb8458)

17. Cooper WE, Vitt LJ. 2002 Distribution, extent, and evolution of plant consumption by lizards. *J. Zool.* **257**, 487–517. (doi:10.1017/S0952836902001085)

18. Meiri S. 2018 Traits of lizards of the world: variation around a successful evolutionary design. *Glob. Ecol. Biogeogr.* **27**, 1168–1172. (doi:10.1111/geb.12773)

19. Szarski H. 1962 Some remarks on herbivorous lizards. *Evolution* **16**, 529–529. (doi:10.2307/2406186)

20. Ostrom JH. 1963 Further comments on herbivorous lizards. *Evolution* **17**, 368–369. (doi:10.2307/2406166)

21. Pough FH. 1973 Lizard energetics and diet. *Ecology* **54**, 837–844. (doi:10.2307/1935678)

22. Hotton III N. 1955 A survey of adaptive relationships of dentition to diet in the North American Iguanidae. *Am. Midl. Nat.* **88**, 114.

23. King GM. 1996 *Reptiles and herbivory*. Berlin, Germany: Springer Science & Business Media.

24. Espinoza RE, Wiens JJ, Tracy CR. 2004 Recurrent evolution of herbivory in small, cold-climate lizards: breaking the ecophysiological rules of reptilian herbivory. *Proc. Natl Acad. Sci. USA* **101**, 16 819–16 824. (doi:10.1073/pnas.0401226101)

25. Lafuma F, Corfe IJ, Clavel J, Di-Poï N. 2021 Multiple evolutionary origins and losses of tooth complexity in squamates. *Nat. Commun.* **12**, 1–13. (doi:10.1038/s41467-021-26285-w)

26. Herrel A. 2007 Herbivory and foraging mode in lizards. In *Lizard ecology: the evolutionary consequences of foraging mode* (eds SM Reilly, LD McBrayer, DB Miles). Cambridge, UK: Cambridge University Press.

27. Nevo E, Gorman G, Soulé M, Yang SY, Clover R, Jovanović V. 1972 Competitive exclusion between insular *Lacerta* species (Sauria, Lacertidae): notes on experimental introductions. *Oecologia* **10**, 183–190. (doi:10.1007/BF00347990)

28. Wehrle BA, Herrel A, Nguyen-Phuc B-Q, Maldonado Jr S, Dang RK, Agnihotri R, Tadic Z, German DP. 2020 Rapid dietary shift in *Podarcis sicula* resulted in localized changes in gut function. *Physiol. Biochem. Zool.* **93**, 396–415. (doi:10.1086/709848)

29. Lemieux-Labonté V, Vigliotti C, Tadic Z, Wehrle B, Lopez P, Bapteste E, Lapointe F-J, German D, Herrel A. 2022 Proximate drivers of population-level lizard gut microbial diversity: impacts of diet, insularity, and local environment. *Microorganisms* **10**, 1550. (doi:10.3390/microorganisms10081550)

30. Taverne M, Dutel H, Fagan M, Štambuk A, Lisicic D, Tadic Z, Fabre A-C, Herrel A. 2021 From micro to macroevolution: drivers of shape variation in an island radiation of *Podarcis* lizards in the Adriatic. *Evolution* **75**, 2685–2707. (doi:10.1111/evo.14326)

31. Herrel A, Spithoven L, Van Damme R, De Vree F. 1999b Sexual dimorphism of head size in *Gallotia galloti*: testing the niche divergence. *Funct. Ecol.* **13**, 289–297. (doi:10.1046/j.1365-2435.1999.00305.x)

32. Rasband WS. 1997 ImageJ. See https://imagej.nih.gov/ij.

33. Mendez J, Keys A. 1960 Density of fat and bone mineral of mammalian muscle. *Metab.-Clin. Exp.* **9**, 184–188.

34. Sellers WI, Crompton RH. 2004 Using sensitivity analysis to validate the predictions of a biomechanical model of bite forces. *Ann. Anat.* **186**, 89–95. (doi:10.1016/S0940-9602(04)80132-8)

35. Gröning F, Jones MEH, Curtis N, Herrel A, O'Higgins P, Evans SE, Fagan MJ. 2013 The importance of accurate muscle modelling for biomechanical analyses: a case study with a lizard skull. *J. R. Soc. Interface* **10**, 20130216. (doi:10.1098/rsif.2013.0216)

36. Kikuchi Y, Kuraoka A. 2014 Differences in muscle dimensional parameters between non-formalin-fixed (freeze-thawed) and formalin-fixed specimen in Gorilla (*Gorilla gorilla*). *Mammal Study* **39**, 65–72. (doi:10.3106/041.039.0101)

37. Taverne M et al. 2020 Proximate and ultimate drivers of variation in bite force in insular lizards *Podarcis melisellensis* and *Podarcis siculus*. *Biol. J. Linnean Soc.* **131**, 88–108. (doi:10.1093/biolinnean/blaa091)

38. Taverne M, Decamps T, Mira O, Sabolic I, da Silva JD, Glogoski M, Lisicic D, Stambuk A, Herrel A. 2022 Relationships between dietary breadth and flexibility in jaw movement: a case study of two recently diverged insular populations of *Podarcis* lizards. *Comp. Biochem. Physiol. - Mol. Integr. Physiol.* **265**, 111140. (doi:10.1016/j.cbpa.2021.111140)

39. Cowin SC. 2001 *Bone mechanics handbook*, 2nd edn. Boca Raton, FL: CRC Press.

40. Rayfield EJ. 2005 Using finite-element analysis to investigate suture morphology: a case study using large carnivorous dinosaurs. *Anat. Rec.* **283A**, 349–365. (doi:10.1002/ar.a.20168)

41. Shannon CE. 1948 A mathematical theory of communication. *Bell Syst. Tech. J.* **27**, 379–423. (doi:10.1002/j.1538-7305.1948.tb01338.x)

42. Herrel A, Aerts P, Fret J, De Vree F. 1999 Morphology of the feeding system in Agamid lizards: ecological correlates. *Anat. Rec.* **254**, 496–507. (doi:10.1002/(SICI)1097-0185(19990401)254:4<496::AID-AR5>3.0.CO;2-Q)

43. Vervust B, Van Dongen S, Grbac I, Van Damme R. 2009 The mystery of the missing toes: extreme levels of natural mutilation in island lizard populations. *Funct. Ecol.* **23**, 996–1003. (doi:10.1111/j.1365-2435.2009.01580.x)

44. Donihue CM, Brock KM, Foufopoulos J, Herrel A. 2016 Feed or fight: testing the impact of food availability and intraspecific aggression on the functional ecology of an island lizard. *Funct. Ecol.* **30**, 566–575. (doi:10.1111/1365-2435.12550)

45. Kolbe JJ, Leal M, Schoener TW, Spiller DA, Losos JB. 2012 Founder effects persist despite adaptive differentiation: a field experiment with lizards. *Science* **335**, 1086–1089. (doi:10.1126/science.1209566)

46. Herrel A, Verstappen M, De Vree F. 1999 Modularity complexity of the feeding repertoire in scincid lizards. *J. Comp. Phys. A* **184**, 501–518. (doi:10.1007/s003590050350)

47. Bjorndal KA, Bolten AB, Moore JE. 1990 Digestive fermentation in herbivores: effect of food particle size. *Physiol. Zool.* **63**, 710–721. (doi:10.1086/physzool.63.4.30158172)

48. Bjorndal KA, Bolten AB. 1992 Body size and digestive efficiency in an herbivorous freshwater turtle: advantages of small bite size. *Physiol. Zool.* **65**, 1028–1039. (doi:10.1086/physzool.65.5.30158557)

49. Taverne M *et al.* 2019 Diet variability among insular populations of *Podarcis* lizards reveals diverse strategies to face resource-limited environments. *Ecol. Evol.* **9**, 12 408–12 420. (doi:10.1002/ece3.5626)

50. Moazen M, Peskett E, Babbs C, Pauws E, Fagan MJ. 2015 Mechanical properties of calvarial bones in a mouse model for craniosynostosis. *PLoS ONE* **10**, e0125757. (doi:10.1371/journal.pone.0125757)

51. Moazen M, Curtis N, O'Higgins P, Jones MEH, Evans SE, Fagan MJ. 2008 Assessment of the role of sutures in a lizard skull: a computer modelling study. *Proc. R. Soc. B* **276**, 39–46. (doi:10.1098/rspb.2008.0863)

52. Costantini D, Alonso ML, Moazen M, Bruner E. 2010 The relationship between cephalic scales and bones in lizards: a preliminary microtomographic survey on three lacertid species. *Anat. Rec.: Adv. Integr. Anat. Evol. Biol.* **293**, 183–194. (doi:10.1002/ar.21048)

53. Jones MEH, Gröning F, Dutel H, Sharp A, Fagan MJ, Evans SE. 2017 The biomechanical role of the chondrocranium and sutures in a lizard cranium. *J. R. Soc. Interface* **14**, 20170637. (doi:10.1098/rsif.2017.0637)

54. Taverne M, Watson PJ, Dutel H, Boistel R, Lisicic D, Tadic Z, Fabre A-C, Fagan MJ, Herrel A. 2023 Data from: Form–function relationships underlie rapid dietary changes in a lizard. Dryad Digital Repository. (doi:10.5061/dryad.866t1g1vk)

55. Taverne M, Watson PJ, Dutel H, Boistel R, Lisicic D, Tadic Z, Fabre A-C, Fagan MJ, Herrel A. 2023 Form–function relationships underlie rapid dietary changes in a lizard. Figshare. (doi:10.6084/m9.figshare.c.6662941)